Electrical and Mechanical Anharmonicities from NIR-VCD Spectra of Compounds Exhibiting Axial and Planar Chirality: The Cases of (*S*)-2,3-Pentadiene and Methyl-d_3 (*R*)- and (*S*)-[2.2]Paracyclophane-4-carboxylate

SERGIO ABBATE,[1,2]* GIOVANNA LONGHI,[1,2] FABRIZIO GANGEMI,[1] ROBERTO GANGEMI,[1,2] STEFANO SUPERCHI,[3] ANNA MARIA CAPORUSSO,[4] AND RENZO RUZZICONI[5]

[1]*Dipartimento di Scienze Biomediche e Biotecnologie, Università di Brescia, Viale Europa 11, 25123 Brescia, Italy*
[2]*CNISM, Consorzio Interuniversitario Scienze Fisiche della Materia, Via della Vasca Navale 84, 00146 Roma, Italy*
[3]*Dipartimento di Chimica, Università della Basilicata, Via dell'Ateneo Lucano, 85100 Potenza, Italy*
[4]*Dipartimento di Chimica e Chimica Industriale, Università di Pisa, Via Risorgimento 35, 56126 Pisa, Italy*
[5]*Dipartimento di Chimica, Università degli Studi di Perugia, Via Elce di Sotto 8, 06123 Perugia, Italy*

Contribution to the Carlo Rosini Special Issue

ABSTRACT The IR and Near infrared (NIR) vibrational circular dichroism (VCD) spectra of molecules endowed with noncentral chirality have been investigated. Data for fundamental, first, and second overtone regions of (*S*)-2,3-pentadiene, exhibiting axial chirality, and methyl-d_3 (*R*)- and (*S*)-[2.2]paracyclophane-4-carboxylate, exhibiting planar chirality have been measured and analyzed. The analysis of NIR and IR VCD spectra was based on the local-mode model and the use of density functional theory (DFT), providing mechanical and electrical anharmonic terms for all CH-bonds. The comparison of experimental and calculated spectra is satisfactory and allows one to monitor fine details in the asymmetric charge distribution in the molecules: these details consist in the harmonic frequencies, in the principal anharmonicity constants, in both the atomic polar and axial tensors and in their first and second derivatives with respect to the CH-stretching coordinates. *Chirality 23:841–849, 2011.*

KEY WORDS: vibrational circular dichroism (VCD); density functional theory (DFT); atomic polar tensors (APT); atomic axial tensors (AAT)

INTRODUCTION

Near infrared (NIR) vibrational circular dichroism (VCD) spectroscopy has been known for many years, since Keiderling and Stephens in 1976 demonstrated the feasibility of NIR-VCD experiments[1] for the first overtone of camphor CH-stretchings. Since then, a systematic investigation of terpene-molecules was carried out in the NIR region, focusing the attention mainly on the second and third overtones of the CH-stretchings.[2] Although the paucity of experimental data, as well as their uncertain interpretation, prevented the use of this valuable tool for several years; recently, the use of more sophisticated instruments,[3–6] conjointly with the development of ab initio calculations of mechanical and electrical anharmonic terms based on the density functional theory (DFT), gave a new impulse for more profitable investigation in this field. This allowed us to reproduce NIR-VCD spectra, thus gaining specific information unattainable by the more widely used IR-VCD technique.[7–9] In general, an approximate but acceptable interpretation of NIR absorption spectra is obtained by assuming the local-mode behavior for X—H stretchings, whose overtone and combination modes contribute in a preponderant way to the NIR spectra.[10] By assuming the local-mode model applicable to NIR-VCD, we were able to acquire important information on the isolated X—H stretching vibrations, by combining NIR-VCD data and ab initio calculations performed with standard computer programs supplemented with our routines.[7,8] For instance, we were able to evidence the quite different spectroscopic behavior not only of the C_4—H bond in camphorquinone with respect to that same bond in camphor but also to highlight the quite different behavior of C_4—H with respect to the other C—H bonds in camphorquinone itself.[3,8] Herein, we wish to pursue a similar investigation on the harmonic and anharmonic features of C—H bonds not only in natural product field but also in ad hoc synthesized compounds endowed with noncentral chirality like (*S*)-2,3-pentadiene, sometimes referred to as (*S*)-(1,3)-dimethylallene, (*S*)-**1** displaying axial chirality and enantiomeric methyl-d_3 (*R*)- and (*S*)-[2.2]paracyclophane-4-carboxylate, (*R*)-**2** and (*S*)-**2** exhibiting planar chirality (see Scheme 1).

Compound **2** was already investigated in our previous work,[11] where we showed that electrical anharmonicity is essential to obtain the correct sign of NIR-VCD bands, although anharmonic contributions from atomic axial tensors (AAT) were disregarded there. New data in the NIR and better protocols for DFT calculations are now available. On the

Additional Supporting Information may be found in the online version of this article.

Contract grant sponsor: Italian "Ministero dell'Istruzione, dell'Università e della Ricerca" (MIUR) (PRIN 2008LYSESR) (which was originally coordinated by Professor Carlo Rosini).

*Correspondence to: Sergio Abbate, Dipartimento di Scienze Biomediche e Biotecnologie, Università di Brescia, Viale Europa 11, 25123 Brescia, Italy.
E-mail: abbate@med.unibs.it

Received for publication 28 February 2011; Accepted 20 July 2011
DOI: 10.1002/chir.21013
Published online 7 September 2011 in Wiley Online Library (wileyonlinelibrary.com).

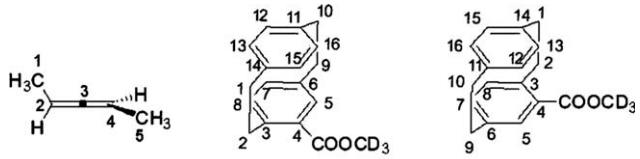

Scheme 1.

contrary, VCD data of the allene (*S*)-**1** were never reported, neither in the mid-IR nor in the NIR region; we remind though that important VCD studies of other substituted allenes in the mid-IR and in the C—H-stretching region were first conducted by Narayanan and coworkers.[12–15] Both molecules present different types of C—H bonds, whose spectroscopic behavior can be easily guessed by a skilled chemist. Nevertheless, we wish to highlight finer details for them, beyond the obvious differences in aliphatic and aromatic C—H bonds. In particular, we will take care in stressing the peculiarity of the NIR-VCD spectra in connection with the molecular chirality.

DESCRIPTION OF EXPERIMENTS AND CALCULATIONS

Sample Preparation

^{1}H and ^{13}C NMR spectra were recorded at room temperature on Varian Gemini 200 and Bruker 400 instruments in $CDCl_3$ solution using $SiMe_4$ as internal standard. Optical rotations were measured with a PerkinElmer 142 automatic polarimeter using standard cuvettes (l = 1 dm). gas-liquid chromatography (GLC) analyses were performed on a PerkinElmer Mod. 5800 instrument equipped with a flame ionization detector and a fused silica capillary column (BP1 bonded, 0.22 mm × 12 m).

(*S*)-2,3-Pentadiene [(*S*)-1]. A sample of (*R*)-(+)-1-butyn-3-ol (**3**), $[\alpha]_D^{25}$ + 42.8 (c = 3.2, dioxane) was obtained by resolution of the corresponding racemic hydrogen phthalate with (*R*)-1-phenylethylamine[16]; its optical purity (*ee* = 82%) was determined by GLC and ^{1}H NMR of the corresponding (*S*)-2-methoxy-2-(trifluoromethyl)phenyl acetate [(*S*)-MPTA Mosher's ester].

A slight excess of methanesulfonyl chloride (22.1 g, 0.19 mol) was added to a well-stirred solution of **3** (9.9 g, 0.14 mol) and triethylamine (21.4 g, 0.21 mol) in dry dichloromethane (485 mL) at –50°C, the cold bath was removed, and the temperature was allowed to rise to 25°C. After further 30 min stirring, water (100 mL) was added, and the mixture was extracted with dichloromethane (3 × 50 mL). The combined extracts were washed with water (2 × 50 mL), dried over Na_2SO_4, and the solvent was evaporated at reduced pressure (20 Torr) affording (*R*)-1-butyn-3-ol methanesulfonate (**4**). The crude methanesulfonyl ester **4** (20.0 g, 0.13 mol, 96%) was then added in 5 min, at –70°C under dry nitrogen atmosphere, to a tetrahydrofurane (THF) solution of methylbromocuprate [(MeCuBr)MgBr.LiBr, 0.270 mol], in turn prepared by adding CH_3MgBr (1 equiv.) to a freshly prepared solution of $LiCuBr_2$ (0.270 mol) in THF at –50°C while stirring. After 30 min, a saturated aqueous NH_4Cl solution (50 mL) was added, and the organic materials were extracted with THF (3 × 50 mL). The collected organic phases were washed with additional aqueous NH_4Cl (2 × 50 mL) and dried with Na_2SO_4. Pure (*S*)-**1** (4.6 g, 50% yield) was recovered by reiterated distillations with a Fischer SPALTROHOR column: b.p. 45°C, d_4^{25} 0.6900, $[\alpha]_D^{25}$ + 68.5, ^{1}H NMR (200 MHz) δ 5.00 (m, 2 H, $CH_3C\underline{H}$=), 1.63 (dd, J = 4.5 and 5.6 Hz, 6 H, $C\underline{H}_3CH$=), ^{13}C NMR (50 MHz) δ 206, 84.7, 14.1.

Methyl-d_3 (*R*)- [(*R*)-2] and (*S*)-[2.2]paracyclophane-4-carboxylate [(*S*)-2]. These compounds were prepared as previously described.[11]

IR and VCD Spectra in the Fundamental Region

(*S*)-2,3-Pentadiene [(*S*)-1]. The spectra of the allene **1** (0.1 M in CCl_4 solution) were registered on a Jasco FVS4000 FTIR instrument using an InSb detector for measurements in the 3300–2700 cm^{-1} fundamental CH-stretching region (1 mm quartz cell), while a HgCdTe detector was used in scanning the 1600–900 cm^{-1} mid-IR region (500 μm BaF_2 cell). Both VCD and IR spectra of the solvent were subtracted. In all cases, the data are an average of 4000 scans, at least.

Methyl-d_3 (*R*)- [(*R*)-2] and (*S*)-[2.2]paracyclophane-4-carboxylate [(*S*)-2]. IR-VCD and IR absorption spectra were taken out of the previous work.[11]

NIR and NIR-VCD Spectra

All NIR spectra, both in absorption (VA) and VCD, were taken with dispersive instruments, which are linear in wavelengths. For a direct comparison of the Δv = 1 data with those of the current literature and to make the discussion easier, the frequency values are reported in wavenumbers.

(*S*)-2,3-Pentadiene [(*S*)-1]. NIR absorption spectra of neat samples of (*S*)-**1** were registered with a UV–vis-NIR CARY 05E instrument using quartz cuvettes of 0.1–1.0 cm pathlengths. They are reported in Figure 1 together with the spectra in the fundamental CH-stretching region. The ϵ values were obtained by referring to a density of 0.7 g cm^{-3}.[17,18] Two bands of almost equal intensity are observed at high overtones (Δv = 3 and Δv = 4), the narrower band at lower energy and the broader one at higher energy. Their harmonic frequencies at ω_{01} = 3063 cm^{-1} and ω_{02} = 3118 cm^{-1} and their anharmonicities, χ_1 = 67 cm^{-1} and χ_2 = 68 cm^{-1}, respectively, were derived from the Birge-Sponer plot.[10]

NIR-VCD spectra were obtained with a home-made apparatus described earlier,[3] with a special procedure for getting rid of baseline artefacts.[19] Neat samples were used for the Δv = 3 region in a 1-mm pathlength cell; CCl_4 solution was used for VCD measurements in the Δv = 2 region. To avoid evaporation of low boiling (*S*)-**1** during NIR absorption and VCD measurements, which take about 10 min, the liquid sample of (*S*)-**1** was transferred at low temperature from the bottle into the cuvettes, and the latter were tightly sealed.

Methyl-d_3 (*R*)- [(*R*)-2] and (*S*)-[2.2]paracyclophane-4-carboxylate [(*S*)-2]. Both the NIR absorption data and the NIR-VCD data for (*S*)-**2** and (*R*)-**2** were taken on our home-made apparatus for measuring NIR VCD spectra. To make easier the comparison between the two molecules, the former spectra from the Supporting Information of Ref. 11 are reported in Figure 2. We observe that, as for compound (*S*)-**1**, two features stand out for Δv = 3 and Δv = 4; their intensity and shape is more similar than those observed for compound (*S*)-**1**, and this makes the local mode hypothesis more tenable, providing ω_{01} = 3045 cm^{-1} and χ_1 = 60.6 cm^{-1} and ω_{02} = 3173 cm^{-1} and χ_2 = 65.4 cm^{-1} for aliphatic and aromatic CH bonds, respectively, according to the Birge-Sponer law. The procedure and conditions for registering NIR-VCD data are described in Ref. 11, except for Δv = 2, for which we use a new extended InGaAs detector.

DFT Calculations

All calculations were run with the Gaussian03 or the Gaussian09 set of programs.[20] The employed functionals/basis sets were: B3LYP and 6-311++G** for (*S*)-**1** and B3LYP and TZVP for (*R*)-**2**. Quite similar results were obtained with other functionals/basis sets. The calculated IR-VCD, Δv = 1 spectra of (*S*)-**1**, never reported before, allowed us to reproduce spectra to compare with experimental ones. The harmonic frequencies and dipole and rotational strengths were obtained with Gaussian (spectra were reconstructed assigning a Lorentzian bandshape of assumed bandwidth ($\Delta\nu$ = 16 cm^{-1} for the CH-stretching region and $\Delta\nu$ = 8 cm^{-1} for the mid-IR) to each vibrational transition). For (*R*)-**2** such data had been already presented in Ref. 11.

The method for calculating NIR and NIR-VCD spectra was illustrated earlier[7–9] and, in practical terms, consists in home-made computer programs that make use of outputs from Gaussian. The procedure is divided in two parts: one concerns the calculation of me-

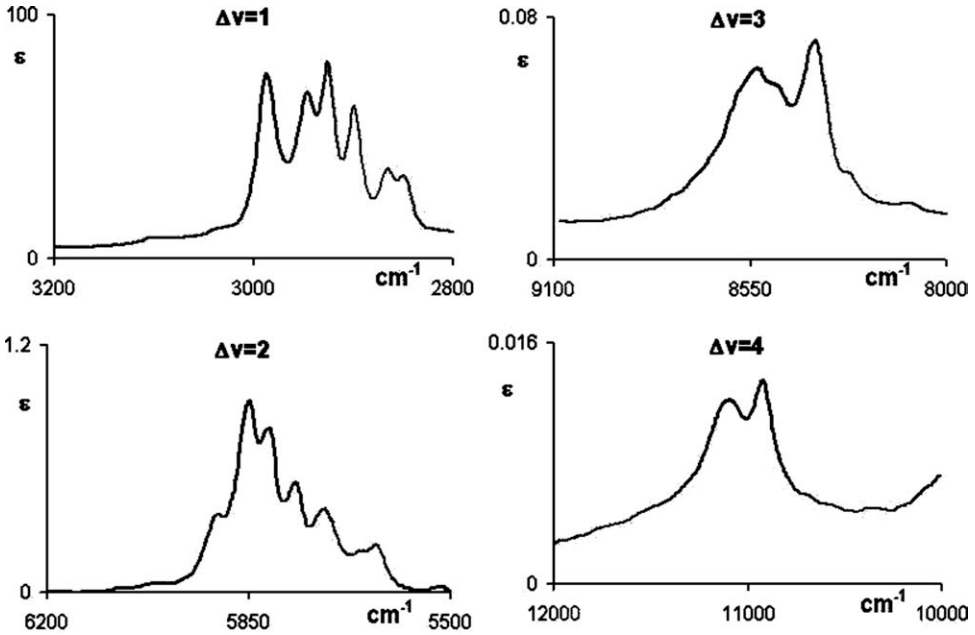

Fig. 1. Experimental CH-stretching fundamental ($\Delta v = 1$) and overtone ($\Delta v = 2, 3, 4$) absorption spectra of (*S*)-2,3-pentadiene ((*S*)-**1**) (ϵ in 10^3 cm^2 mol^{-1}).

chanical harmonic frequencies ω_0 and anharmonicities χ (local-mode mechanical terms); the other concerns the calculation of atomic polar tensors (APT), atomic axial tensors (AAT) and their first and second derivatives with respect to C—H stretchings (local mode electrical anharmonicities).[7,8] The calculation of mechanical terms is based on a numerical approach proposed by Henry and Kjaergaard,[21] while that of the electrical anharmonicities goes by an idea of Bak et al.,[22] that, in turn, bases itself on the theory of Stephens[23] and of Buckingham et al.[24] This approach allows one to calculate, without approximations except the local-mode assumption, the frequencies for the overtone transitions of all CH-stretchings by the Birge-Sponer law:

$$\omega_v = (\omega_0 - \chi)v - \chi v^2 \quad (1)$$

as well as their dipole strengths and rotational strengths using Morse transition integrals and calculated APT and AAT characteristics. Finally, as in the IR case, we assume Lorentzian bandshapes, to facilitate comparison of experimental and calculated data, with empirical values for $\Delta\omega$ for each CH-stretching region.

RESULTS AND DISCUSSION

(S)-2,3-Pentadiene

A sample of allene (*S*)-**1** was obtained as described above according to the general procedure developed by Elsevier and Vermeer for the synthesis of optically active allenes (Scheme 2).[25]

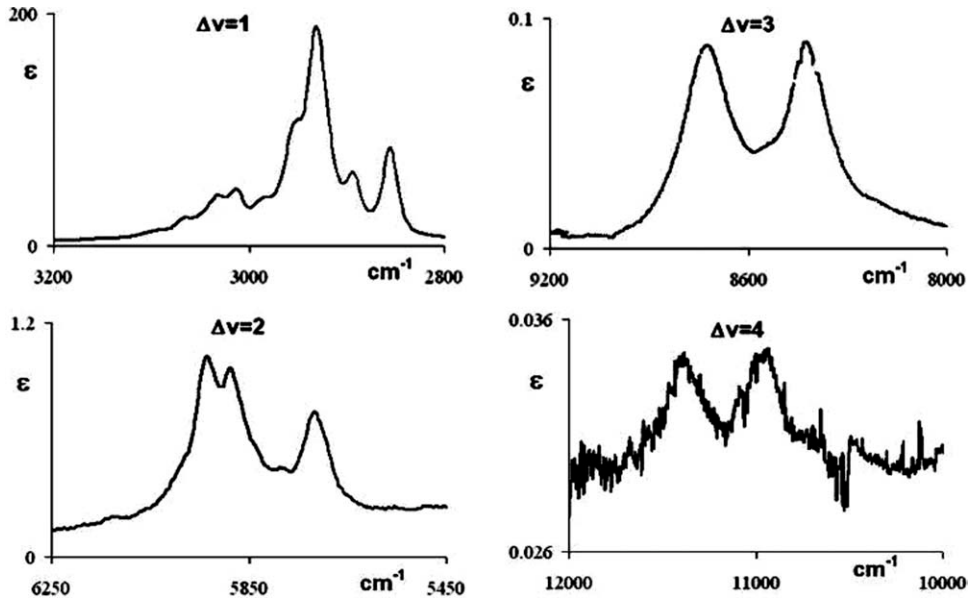

Fig. 2. Experimental CH-stretching fundamental ($\Delta v = 1$) and overtone ($\Delta v = 2, 3, 4$) absorption spectra of methyl-d_3 (*S*)-[2.2]paracyclophane-4-carboxylate ((*S*)-**2**). The poor signal-to-noise ratio at $\Delta v = 4$ is due to the little quantity of sample used in taking the spectrum. (ϵ in 10^3 cm^2 mol^{-1}).

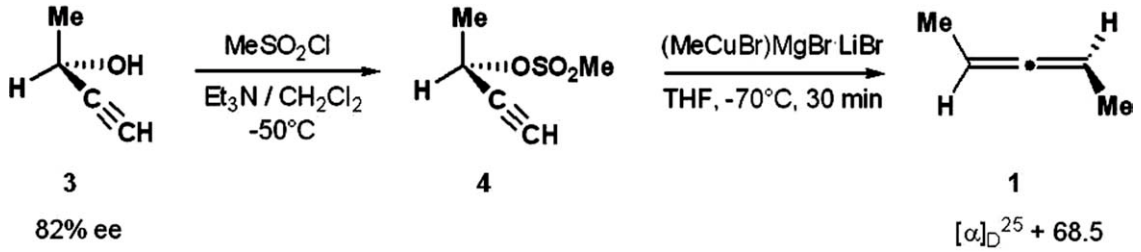

Scheme 2.

Thus, enantiomerically enriched (*R*)-1-butyn-3-ol (**3**), obtained with 82% *ee* by resolution of its hydrogen phthalate with (*R*)-1-phenylethylamine,[16] was quantitatively converted into the methanesulfonate **4** by reaction, at –50°C in dichloromethane, with methanesulfonyl chloride and triethylamine. The crude compound **4** reacts nicely with the complex organocopper reagent (MeCuBr)MgBr.LiBr, prepared in THF from MeMgBr and $LiCuBr_2$, affording the dimethylallene (*S*)-**1** with good yield through a stereoselective 1,3-anti-substitution. As it was checked that substrates and products retain their stereochemical integrity under reaction conditions,[25] compound (*S*)-**1** should be recovered with a high optical yield. In fact, we can attribute to (*S*)-**1**, having $[\alpha]_D^{25}$ + 68.5 (Scheme 2), an enantiomeric excess of about 79% taking into account the molar rotation ϕ_D which can be calculated for this compound by the semiempirical Runge's rule.[18,26]

The comparison between calculated and experimental IR and mid-IR absorption and VCD spectra is given in Figure 3: 3-right referring to the C—H stretching fundamental region (3200–2800 cm^{-1}) and 3-left to fundamentals of bending and C—C stretchings (1600–920 cm^{-1}). Keeping in mind that the DFT calculations are run in this case at the harmonic level, the results may be considered satisfactory, particularly in the mid-IR (Figure 3-left). The molecule exists in just one conformation and exhibits fairly well defined features. Modest broadening is possibly brought in by methyl hindered torsion. The results in this region allow confirmation of the absolute configuration (*S*) of the dimethylallene **1**. By contrast, the results of the C—H stretching fundamental region (Figure 3-right) show off the effects of disregarding the anharmonicity (including Fermi resonance, as in Ref. 11). However, the succession of the calculated VCD features is reminiscent of the observed VCD spectrum. Analogies with previous VCD works in both mid-IR and C—H stretching region for other substituted allenes can be found by comparing the present results with those of Refs. 12–15.

The DFT calculated values of ω_0 and χ for inequivalent C—H bonds and, for sake of comparison, the corresponding "experimental" values derived from the Birge-Sponer plots are reported in Table 1. While the χ values are quite similar, ω_0 values change remarkably from bond to bond, the highest ω_0 values being assigned to the olefinic C—H and to the methyl C—H bonds lying in the C=C—C plane. This could mean that a residual double bond character is exhibited through that plane C_{sp}–C_{sp2}–C_{sp3}, while the other two methyl C—H bonds exhibit a more aliphatic character. We conclude that hyperconjugation keeps all ω_0 values of C—H bonds close to each other and the drastic differentiation between

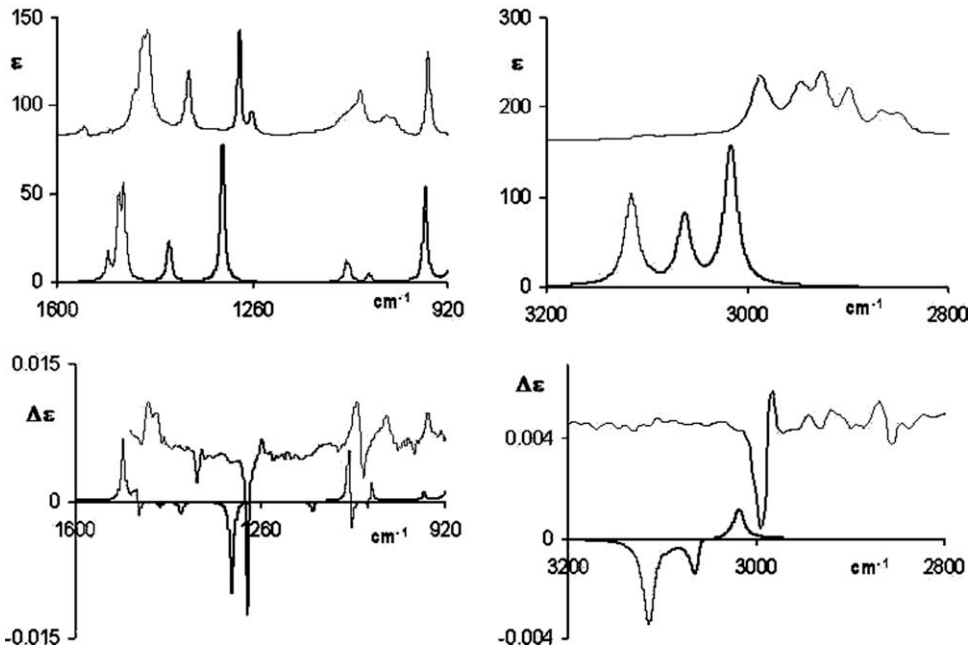

Fig. 3. Comparison of calculated (black) and experimental (grey) absorption and VCD spectra of (*S*)-2,3-pentadiene ((*S*)-**1**) for the mid-IR deformation/bending region (first column) and for the fundamental CH-stretching region (second column). Calculations are run in the harmonic approximation (*i.e.* are not shifted to account for anharmonicity), with Gaussian[20] and a 6-311++g(d,p) basis/B3LYP functional.

TABLE 1. (*S*)-2,3-Pentadiene ((*S*)-1): calculated harmonic frequencies (ω_0) and anharmonicities (χ) (cm^{-1}) by the method illustrated in Ref. 9 for inequivalent CH bonds (see Scheme 1)

			Experimental		$\partial\mu_z/\partial z$ (APT)	$\partial^2\mu_z/\partial z^2$ (APT')	$\partial^3\mu_z/\partial z^3$ (APT")	$\partial m_x/\partial p_z$ (AAT)	$\partial^2 m_x/\partial z\partial p_z$ (AAT')	$\partial^3 m_x/\partial z^2\partial p_z$ (AAT")
Bond	ω_0	χ	ω_0	χ	z-Components					
C_1Hop	3049	60.0	3063	67	−0.1636	−0.6386	−0.3724	0.2381	0.5837	0.0623
C_1Hop'	3044	59.8			−0.1712	−0.6674	−0.3946	0.2045	0.4570	−0.0249
C_1Hip	3103	59.8	3118	68	−0.1114	−0.3872	0.0385	0.2150	0.6183	−0.1100
C_2H	3099	60.7			−0.1073	−0.6547	−0.7624	0.0999	0.3504	0.4750

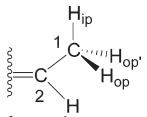

Corresponding experimental values derived on the basis of IR and NIR absorption spectra (see text). The zz components of APT (e) and xz of AAT ($ea_0/\hbar c$) and their derivatives calculated at equilibrium (see Supporting Information Figure SI-1). Calculation method: B3LYP/6-311++g(d,p) (e is the electronic charge, a_0 is the Bohr's radius, $\hbar$ is the reduced Planck's constant, c is the speed of light).

olefinic and aliphatic CHs is not substantial. We now wish to compare these values for ω_0 and χ with the experimental values of ω_0 and χ: by the latter, we mean the values obtained by using in the Birge-Sponer eq. 1 the experimental values for ω_v for $v = 1, 2, 3, 4$, and so on.[10,27] A least squares statistical fit is used to derive the values for the two parameters ω_0 and χ from experimental frequencies. In this case, we used the values ω_v, which we read in Figure 1. We find that the experimental values for ω_0 and χ are larger than the calculated ones. This outcome could be attributed to some plausible deviation from the local-mode behavior; in particular, we think that the broader, high-wavenumber features might include combination modes that do not suit the present model, as they appear at frequencies higher than pure overtones; anyway, a basis set and/or a solvent effect may also play some role.

The dependence of APT and AAT (i,z) components (i = x,y,z) of all inequivalent hydrogen atoms on the C—H stretching lengths, as calculated by our method,[7–9] is shown in Figure SI-1 of the Supporting Information file. The first and second derivatives with respect to (z) C—H stretching of the APT z-component and the AAT x-component (which are the largest ones) at equilibrium are reported in Table 1 (local axes are chosen as follows: the z-axis is along the C—H bond under examination, the y-axis is in the H-C-C plane and x perpendicular to it[7,9]). The APT values at equilibrium are similar to those we calculated previously for camphor,[8] while their first derivatives are slightly higher in absolute value, except for the olefinic C—H bond, which shows a quite small APT first derivative. Large values of AAT in the x-direction at equilibrium as well as those of their derivatives, entail large circulations of charge (due to the CH-stretching) in the C=C—C plane. While the NIR absorption spectra are determined by the z-component of APTs, the x-component of AAT (together with the x-component of APT) largely determines the NIR-VCD spectra. From these and from the analogous parameters for the corresponding bonded carbon atom,[7,8] we deduced the calculated VCD and absorption spectra ab initio for $\Delta v = 1$, 2, and 3 (Figure 4). In the latter figure, a comparison with the corresponding experimental data is provided. It should be remembered that, here, the $\Delta v = 1$ is also calculated in the local-mode approximation, while the results at $\Delta v = 1$ for the normal mode case are reported in Figure 3. Let us comment results from each spectroscopic region: it is known that at $\Delta v = 1$, the local-mode approach is in general worse than the normal-mode one, and only the frequency range is much better estimated, as anharmonicity is taken in some consideration. From these results, it may be inferred that the VCD spectrum in the C—H stretching region contains the contributions of two couplets that are resolved in the experiments but not in the calculations of Figure 4. The two VCD couplets are in correspondence with the two calculated absorption bands. The first couplet at higher frequencies, coming from in-plane C—H bond stretchings, provides for a broad absorption and a VCD (−,+) doublet (starting from high-frequency values). The second couplet coming from the out-of-plane C—H bond stretchings, shows a broad and structured absorption and a quite weak (+,−)VCD couplet. Even calculations in the normal-mode scheme do not reproduce faithfully the observed features (Figure 3), and this fact strongly suggests the possible existence of Fermi resonances, especially in the absorption case. The $\Delta v = 2$ region is a transitional region from normal-mode to local-mode regime,[28] and, thus, it is notoriously difficult to reproduce both in the normal-mode and in the local-mode schemes. In facts, contrary to the calculations, which predict just two absorption bands and a large negative VCD feature, the absorption spectrum is rich in combination bands, the NIR-VCD spectrum is positive and weak. On the contrary, at $\Delta v = 3$, where the local-mode behavior is generally fully operative,[10] we have a very good correspondence between experiments and calculations. We are unable to reproduce the broadness of the lower wavelength band, and this is still due to the local-mode approximation. Nevertheless, intensities are in the right range and, most importantly, we attain the interpretation of the VCD data, and we can certainly state that the most intense, negative feature is due to the olefinic CHs. These bonds, very close to the origin of axial chirality, behave similarly to the C_4—H in camphorquinone, which has been shown to be responsible for the high overtone vibrational optical activity of this molecule and is close to two C=O double bonds (cfr. also the APT and AAT values).

Methyl-d_3 (R)- [(R)-2] and (S)-[2.2]Paracyclophane-4-carboxylate [(S)-2]

The comparisons of IR and mid-IR absorption and VCD spectra were presented in Ref. 11 and were quite good as for **1**. For (*R*)-**2** two conformations were predicted by B3LYP/

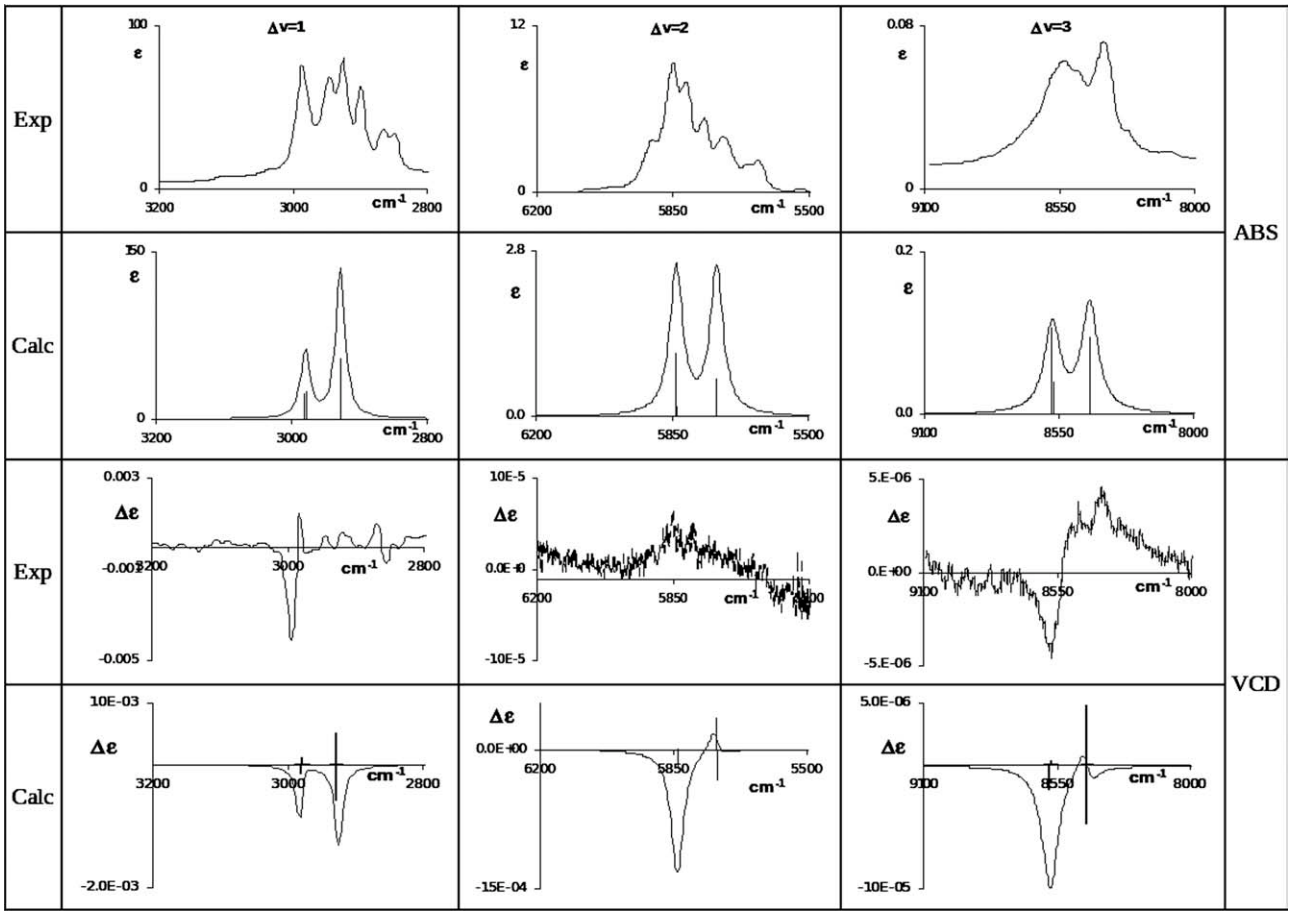

Fig. 4. (*S*)-2,3-pentadiene: Comparison of calculated and experimental IR and NIR absorption (top) and VCD spectra. Left: $\Delta v = 1$, CH-stretching fundamental region (assumed bandwidth in the calculations (HWHM) $\Delta\omega = 8$ cm^{-1}). Center: $\Delta v = 2$, CH-stretching first overtone region (assumed bandwidth in the calculations, HWHM, $\Delta\omega = 20$ cm^{-1}). Right: $\Delta v = 3$, CH-stretching second overtone region (HWHM, $\Delta\omega = 40$ cm^{-1}).

TZVP set with a 84:16 population ratio. The most populated conformer exhibits the C=O bond facing the ethylenic bridge and the OCD_3 in the opposite side; vice versa holds for the less populated conformer. The results for the mid-IR and CH-stretching region are not reported here, and the interested reader should consult Ref. 11. As anharmonic calculations for the NIR region are pretty time-consuming, only the most populated conformer was considered.

In Table 2, we report, together with other data, the calculated values of ω_0 and χ for C—H bonds and compare them with the corresponding "experimental" values, derived, as explained above, from eq. 1 and the spectra of Figure 2. The calculated values for χ and ω_0 are different for aromatic and aliphatic CHs and similar to those obtained for ethyl benzene[11] and toluene[29] by experimental NIR absorption spectroscopy. They are also similar to the values derived by the Birge-Sponer plot (Table 2). However, while the values for χ are very similar, a variety of ω_0 values are noticed, both in the aromatic and in the aliphatic moiety. We find larger ω_0 (of the order of $\approx$3170 cm^{-1}) for aromatic C—H bonds in the ring containing the substituent $COOCD_3$, especially for the C—H at position 5 (3205 cm^{-1}). In the aliphatic region, we also find larger ω_0 for the CH_2CH_2 group closer to the substituent. Among them, two bonds have $\omega_0 \geq 3100$ cm^{-1}, while for the other aliphatic CHs, $\omega_0 \leq 3080$ cm^{-1}. The $COOCD_3$ group, that induces the chirality in the system, seems to determine in large extent also the electric characteristics of the molecule, as we will comment immediately below.

In Figure SI-2 of the Supporting Information file, we have plotted the calculated dependence of APT and AAT (i,z) components ($i = x, y, z$) of the hydrogen atoms on the C—H stretching lengths (local bond axes chosen as for (*S*)-**1**). The first and second derivatives of these curves at equilibrium for APT-zz, together with the derivatives of largest AAT components (y) with respect to z are reported in Table 2, in correspondence with the calculated values of ω_0 and χ. Let us consider the values and first derivatives of the z component of hydrogens' APT with respect to the CH-bond lengths l: they coincide with $(\partial\mu/\partial l)$ and $(\partial^2\mu/\partial l^2)$ previously calculated by the more primitive approach of Ref. 11, and with the same quantities derived by experimental NIR absorption data in Ref. 29. As in the earlier literature,[29] we find that the values $(\partial\mu/\partial l) = APT_{zz}(H)$ of both aromatic and aliphatic CHs are negative, and those of aromatic CHs are smaller in absolute value, reaching a minimum of about -0.02 e for H(5), while the aliphatic APT range from -0.1 e to about -0.15 e, with the exception of H(1) and H(2), which are close to -0.08 e. Noteworthy, H(5), H(1), and H(2) are all close to the stereogenic substituent group $COOCD_3$. A similar trend is observed for $(\partial^2\mu/\partial l^2) = (\partial APT_{zz}(H)/\partial l)$. Differently from compound (*S*)-**1**, both the x and y components of AAT are large and important.

TABLE 2. Methyl-d_3 (*R*)-[2.2]paracyclophane-4-carboxylate ((*R*)-2): calculated harmonic frequencies (ω_0) and anharmonicities (χ) (cm^{-1}) by the method illustrated in Ref. 9 for all CH bonds (see Scheme 1)

				$\frac{\partial \mu_z}{\partial z}$ (APT)	$\frac{\partial^2 \mu_z}{\partial z^2}$ (APT')	$\frac{\partial^3 \mu_z}{\partial z^3}$ (APT")	$\frac{\partial m_y}{\partial p_z}$ (AAT)	$\frac{\partial^2 m_y}{\partial z \partial p_z}$ (AAT')	$\frac{\partial^3 m_y}{\partial z^2 \partial p_z}$ (AAT")
	Bond	ω_0	χ	z-Components					
Aliph	1	3106	61	−0.0935	−0.3959	−0.2540	−0.1884	−0.6153	−0.1889
	1′	3065	62	−0.1825	−0.6561	−0.4566	0.1363	0.2486	0.0050
	2	3123	60	−0.0768	−0.4204	−0.3828	−0.1046	−0.5250	−0.3223
	2′	3072	62	−0.1620	−0.5437	−0.3390	0.2455	0.6493	0.1020
Arom	5	3205	57	−0.0250	−0.3274	−0.4297	−0.0842	−0.3500	−0.0980
	7	3171	59	−0.0919	−0.5136	−0.4304	−0.1233	−0.4374	−0.0756
	8	3174	59	−0.0909	−0.4803	−0.4497	−0.1203	−0.4280	−0.1530
Aliph	9	3070	61	−0.1711	−0.6311	−0.4887	−0.1886	−0.5074	−0.0716
	9′	3079	62	−0.1341	−0.4871	−0.3344	0.3023	0.9340	0.3564
	10	3065	62	−0.1639	−0.6082	−0.4765	−0.2870	−0.8582	−0.2985
	10′	3076	61	−0.1509	−0.5363	−0.3635	0.2208	0.6500	0.1349
Arom	12	3166	59	−0.0999	−0.4975	−0.4852	−0.1704	−0.6040	−0.3030
	13	3164	59	−0.0985	−0.4918	−0.4542	0.1699	0.6237	0.2811
	15	3174	58	−0.0808	−0.4237	−0.3679	0.1407	0.6348	0.4112
	16	3165	59	−0.0966	−0.4707	−0.4310	0.1777	0.6671	0.3523
	Experimental								
	Aromatic	3173	65						
	Aliphatic	3045	61						

Corresponding experimental values derived on the basis of IR and NIR absorption spectra (see text). The zz components of APT (e) and yz of AAT ($ea_0/\hbar c$) and their derivatives calculated at equilibrium (see Supporting Information Figure SI-2). Calculation method: B3LYP/TZVP (e is the electronic charge, a_0 is the Bohr's radius, $\hbar$ is the reduced Planck's constant, c is the speed of light).

Figure 5 shows the absorption and VCD spectra calculated on the basis of the quantities just commented for $\Delta v = 1$, 2, and 3. By comparing them with the corresponding experimental data (the $\Delta v = 1$ calculated results in Figure 5 are in the local mode approximation, while the full normal mode calculations by Gaussian plus discussion on the possible role of Fermi Resonance is given in Ref. 10), we may conclude that in this case, the results are slightly better than for (*S*)-**1**. In particular, they allow understanding why the aromatic region presents very low intensity in absorption and is nearly absent in VCD spectra of the fundamental ($\Delta v = 1$ region), while it is as intense as, or even more intense than, the aliphatic region for $\Delta v \geq 2$. This has been known since long in absorption spectroscopy[29] and it was clarified in 2007 for VCD[11] as being due to the nonlinear dependence of electric and magnetic dipole moment on C—H stretching coordinates. Coming to the details of the various Δv regions, we may say the following: at $\Delta v = 1$ the local-mode approach is worse than obtained directly by the Gaussian harmonic calculations, except that the frequency range is better estimated, since some mechanical anharmonicity is taken into account (below 2900 cm^{-1} another anharmonic phenomenon, i.e., Fermi resonance, is present, but it is not considered here[11]). In the case of (*R*)-**2**, the $\Delta v = 2$ region is simpler than for (*S*)-**1**: the experimental absorption spectrum consists of three features and the calculations provide two major but quite structured bands, since a large variety of aromatic CH, as well as aliphatic CH overtones, the ones close to the substituent and "bordering" the aromatic CHs have to be considered. It is possible that combination modes add to this scheme. The calculated VCD spectrum compares reasonably with the experimental one, better than for allene (*S*)-**1**. This proves that, in this case, the local-mode approximation works better on a large variety of different types of local CHs and produces the structuring of the VCD spectra. Most important, the succession for convoluted calculated bands (+,−,−) is in correspondence with the observed features for (*R*)-**2**. At $\Delta v = 3$, where the local-mode behavior is fully operative,[10] the two main absorption bands, with approximately equal intensities, are attributed to aromatic and aliphatic CHs in a ratio equal to the number of aromatic and aliphatic C—H bonds (7:8). Additionally, minor features are predicted between the two major bands, as observed: this is originated by the unequal distribution of CH-stretching frequencies. Finally, the experimental $\Delta v = 3$ NIR-VCD spectrum consisting of two doublets of (oppositely) alternating signs is interpreted as due to the local modes. Starting from high frequencies, the contributions of aromatic CHs for the bonds close to the $COOCD_3$ substituent (positive intense VCD for (*R*)-**2**) come first, followed by those of the other aromatic CHs (negative intense VCD). The less intense doublet at lower wavenumbers is due to aliphatic CHs, the largest frequency component among the latter being due to aliphatic CHs close to carboxylate group. The present calculations do not account for the last component of the observed couplet.

SUMMARY AND CONCLUSIONS

In this work, we have reported on the CH-stretching fundamental and first two overtone vibrational absorption (VA) and VCD spectra of (*S*)-2,3-pentadiene [alias (*S*)-(1,3)-dimethylallene] (**1**) and of methyl-d_3 (*R*)- and (*S*)-[2.2]paracyclophane-4-carboxylate (**2**), spanning from the standard IR into the NIR region. We have also reported mid-IR VA and VCD spectra of allene **1**, and we provide the harmonic and anharmonic calculations of their spectra. The anharmonic calculations highlight interesting features in the previously neglected parts of the spectra, providing insight into the behavior of APT and AAT of different CH bonds in the molecule: quite different parameters are indeed calculated for CHs next or away from the stereogenic part of the molecules and this difference permits to rationalize the observed NIR-

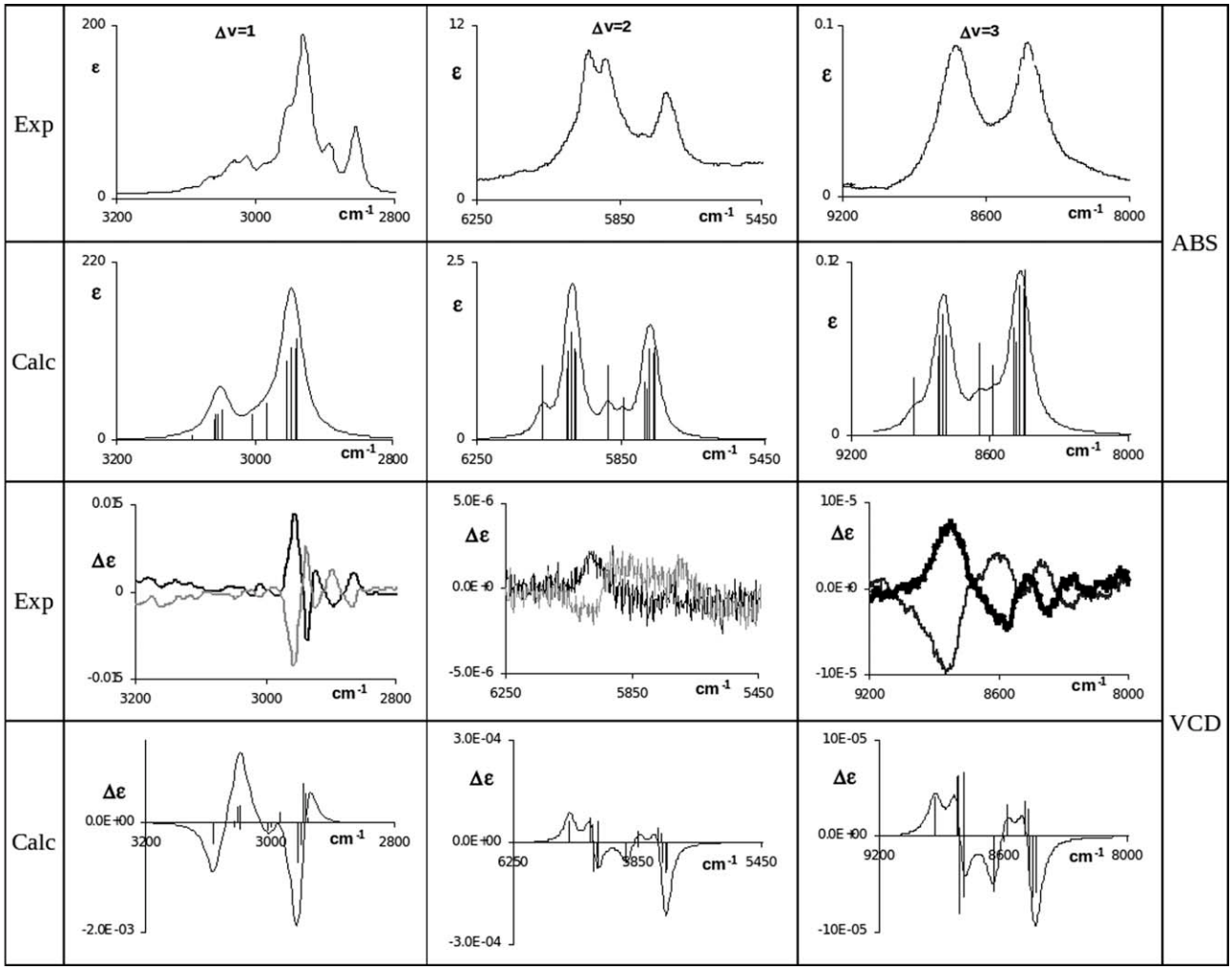

Fig. 5. Methyl-d_3 [2.2]paracyclophane-4-carboxylate. Comparison of experimental IR and NIR absorption (top) and VCD spectra of both enantiomers (R, in black, and S, in gray) with the corresponding calculated spectra for the (*R*)-enantiomer. Left: $\Delta v = 1$, CH-stretching fundamental region (assumed bandwidth in the calculations, (HWHM) $\Delta\omega = 16\ cm^{-1}$). Center: $\Delta v = 2$, CH-stretching first overtone region (assumed bandwidth in the calculations, HWHM, $\Delta\omega = 20\ cm^{-1}$). Right: $\Delta v = 3$, CH-stretching second overtone region (HWHM, $\Delta\omega = 40\ cm^{-1}$).

VCD spectra. We think that the local-mode model works better for **2** than for **1**. In any case, at $\Delta v = 3$, the calculations based on this model work fine on quantitative grounds for both molecules, as well as in other cases.[7–9]

Previous calculations of NIR VA and NIR VCD spectra concerned molecules with a stereogenic carbon atom; in the present case, where other types of chirality are considered, namely the axial and planar ones, we were able to obtain results of similar quality and could also define how parameters such as ω_0, APTs, AATs, as well as their derivatives with respect to local mode stretching for bonds or atoms in the vicinity of the chirality source, are characteristically affected.

ACKNOWLEDGMENTS

Professor Rosini proposed and inspired part of this work but prematurely and unfortunately passed away last year. The Researchers from Brescia thank CILEA (Consorzio Interuniversitario Lombardo Elaborazione Automatica) for access to their computational facilities.

LITERATURE CITED

1. Keiderling TA, Stephens PJ. Vibrational circular dichroism of overtone and combination bands. Chem Phys Lett 1976;41:46–48.
2. Abbate S, Longhi G, Ricard L, Bertucci C, Rosini C, Salvadori P, Moscowitz A. Vibrational circular dichroism as a criteria for local-mode versus normal-mode behavior. Near-infrared circular dichroism of some monoterpenes. J Am Chem Soc 1989;111:836–840.
3. Castiglioni E, Lebon F, Longhi G, Abbate S. Vibrational circular dichroism in the near infrared: instrumental developments and applications. Enantiomer 2002;7:161–173.
4. Cao X, Shah RD, Dukor RK, Guo C, Freedman TB, Nafie LA. Extension of Fourier transform vibrational circular dichroism into the near-infrared region: continuous spectral coverage from 800 to 10000 cm^{-1}. Appl Spectrosc 2004;58:1057–1064.
5. Guo C, Shah RD, Dukor RK, Freedman TB, Cao X, Nafie LA. Fourier transform vibrational circular dichroism from 800 to 10,000 cm^{-1}: near-ir-VCD spectral standards for terpenes and related molecules. Vibr Spectrosc 2006;42:254–272.
6. Ma S, Freedman TB, Dukor RK, Nafie LA. Near-infrared and mid-infrared vibrational circular dichroism of proteins in aqueous solution. Appl Spectrosc 2010;64:615–626.
7. Gangemi F, Gangemi R, Longhi G, Abbate S. Experimental and ab initio calculated spectra of the first OH-stretching overtone of (1R)-(-)-endo-borneol and (1S)-(+)-endo-borneol. Phys Chem Chem Phys 2009;11:2683–2689.
8. Gangemi F, Gangemi R, Longhi G, Abbate S. Calculations of overtone NIR and NIR-VCD spectra of camphor and camphorquinone in the local mode approximation. Vibr Spectrosc 2009;50:257–267.
9. Abbate S, Castiglioni E, Gangemi F, Gangemi R, Longhi G. NIR-VCD, vibrational circular dichroism in the near-infrared: experiments, theory and calculations. Chirality 2010;21:E242–E252.

10. Henry BR. The local mode model and overtone spectra: a probe of molecular structure and conformation. Acc Chem Rev 1987;20: 429–435.
11. Abbate S, Castiglioni E, Gangemi F, Gangemi R, Longhi G, Ruzziconi R, Spizzichino S. Harmonic and anharmonic features of IR and NIR absorption and VCD spectra of chiral 4-X-[2.2]paracyclophanes. J Phys Chem A 2007;111:7031–7040.
12. Narayanan U, Keiderling TA, Elsevier C, Vermeers P, Runge W. Vibrational circular dichroism of optically active substituted allenes. Experimental results. J Am Chem Soc 1988;110:4133–4138.
13. Narayanan U, Keiderling TA. Vibrational circular dichroism of optically active substituted allenes. Calculational results. J Am Chem Soc 1988;110:4139–4144.
14. Narayanan, U, Annamalai, A, Keiderling, TA. Vibrational spectra of 1,3-dideuterioallene and normal mode calculations for allene. Spec Acta 1988:44A;785–791.
15. Annamalai A, Narayanan U, Tissot M-C, Keiderling TA, Jalkanen K, Stephens PJ. Vibrational circular dichroism of 1,3-d2-allene. A calculational study. J Phys Chem 1990;94:194–199.
16. Weidman R, Schoofs A, Horeau A. Effets stériques et éléctroniques dans la méthode du dédoublement partiel de l'anhydride α-phénylbutyrique par les alcools secondaires chiraux – XI. Cas des carbinols α-acétyléniques et α-vinyliques. Bull Soc Chim France 1976:645–648.
17. Doering WvE, LaFlamme PM, A two-step synthesis of allenes from olefins. Tetrahedron 1958;2:75–79.
18. Pomerantz P, Fookson A, Mears TW, Rothberg S, Howard FL. Synthesis and physical properties of several aliphatic and alicyclic hydrocarbons. J Res Natl Bur Stand 1954;52:59–65.
19. Longhi G, Gangemi R, Lebon F, Castiglioni E, Abbate S, Pultz VM, Lightner DA. A comparative study of overtone CH-stretching vibrational circular dichroism spectra of fenchone and camphor. J Phys Chem A 2004;108:5338–5352.
20. Frisch MJ, Trucks GW, Schlegel HB, Scuseria GE, Robb MA, Cheeseman JR, Montgomery JA Jr, Vreven T, Kudin KN, Burant JC, Millam JM, Iyengar SS, Tomasi J, Barone V, Mennucci B, Cossi M, Scalmani G, Rega N, Petersson GA, Nakatsuji H, Hada M, Ehara M, Toyota K, Fukuda R, Hasegawa J, Ishida M, Nakajima T, Honda Y, Kitao O, Nakai H, Klene M, Li X, Knox JE, Hratchian HP, Cross JB, Bakken V, Adamo C, Jaramillo J, Gomperts R, Stratmann RE, Yazyev O, Austin AJ, Cammi R, Pomelli C, Ochterski JW, Ayala PY, Morokuma K, Voth GA, Salvador P, Dannenberg JJ, Zakrzewski VG, Dapprich S, Daniels AD, Strain MC, Farkas O, Malick DK, Rabuck AD, Raghavachari K, Foresman JB, Ortiz JV, Cui Q, Baboul AG, Clifford S, Cioslowski J, Stefanov BB, Liu G, Liashenko A, Piskorz P, Komaromi I, Martin RL, Fox DJ, Keith T, Al-Laham MA, Peng CY, Nanayakkara A, Challacombe M, Gill PMW, Johnson B, Chen W, Wong MW, Gonzalez C, Pople JA. Gaussian 09. Gaussian Inc.: Pittsburgh, PA, 2009.
21. Kjaergaard HG, Henry BR. The relative intensity contributions of axial and equatorial CH bonds in the local mode overtone spectra of cyclohexane. J Chem Phys 1991;96:4841–4851.
22. Bak KL, Bludskỳ O, Jørgensen P. Ab initio calculations of anharmonic vibrational circular dichroism intensities of trans-2,3-dideuterio-oxirane. J Chem Phys 1995;103:10548–10555.
23. Stephens PJ. The theory of vibrational circular dichroism. J Phys Chem 1985;89:748–750.
24. Buckingham AD, Fowler PW, Galwas AP. Velocity-dependent property surfaces and the theory of vibrational circular dichroism. Chem Phys 1985;112:1–14.
25. Elsevier CJ, Vermeer P. Highly stereoselective synthesis of chiral allenes by organocopper(I)-induced anti 1,3-substitution of chiral propynyl esters. J Org Chem 1989;54:3726–3730.
26. Elsevier CJ, Vermeer P, Runge W. Optical rotations of open-chain allenes revisited. Israel J Chem 1985;26:174–180.
27. Abbate S, Longhi G, Castiglioni E. Near infrared vibrational circular dichroism: NIR-VCD, Comprehensive Chiroptical Spectroscopy. In: Berova N, Nakanishi K, Polavarapu PL, Woody RA, editors. Near infrared vibrational circular dichroism: NIR-VCD. New York: Wiley. in press, Chapter 11.
28. Longhi G, Abbate S, Zagano C, Botto G, Ricard-Lespade L. Analysis of the transition from normal modes to local models in a system of two harmonically coupled morse oscillators. Theor Chim Acta 1992;82:321–331.
29. Longhi G, Zerbi G, Ricard L, Abbate S. Electric dipole moment functions from vibrational absorption intensities of fundamental and overtone transitions. J Chem Phys 1988;88:6733–6741.